Synthesis, Photophysics, and Electroluminescence of New Quinoxaline-Containing Poly(p-phenylenevinylene)s

ARTICLE *in* MACROMOLECULES · SEPTEMBER 2004

Impact Factor: 5.8 · DOI: 10.1021/ma048903q

3 AUTHORS, INCLUDING:

John A Mikroyannidis
University of Patras
277 PUBLICATIONS **3,810** CITATIONS
SEE PROFILE

Ioakim K. Spiliopoulos
Technological Educational Institute of Pelop…
40 PUBLICATIONS **851** CITATIONS
SEE PROFILE

Synthesis, Photophysics, and Electroluminescence of New Quinoxaline-Containing Poly(*p*-phenylenevinylene)s

Panayiotis Karastatiris, John A. Mikroyannidis, and Ioakim K. Spiliopoulos*

Chemical Technology Laboratory, Department of Chemistry, University of Patras, Patras, Greece 26500

Abhishek P. Kulkarni and Samson A. Jenekhe*

Departments of Chemical Engineering and of Chemistry, University of Washington, Seattle, Washington 98195

Received June 3, 2004; Revised Manuscript Received August 5, 2004

ABSTRACT: Four new soluble poly(*p*-phenylenevinylene) (PPV) derivatives containing one or two quinoxaline moieties per repeat unit, either in the main chain or as pendants to the main chain, were synthesized, characterized, and explored as emissive and electron transport materials in polymer light-emitting diodes (LEDs). Polymers containing one quinoxaline moiety per repeat unit (**QXPV1** and **QXPV3**) showed low melting transitions (<100 °C), whereas those with two quinoxaline moieties per repeat unit (**QXPV2** and **QXPV4**) had relatively high glass transition temperatures (>140 °C). The polymers emit blue to green light (404−536 nm) in dilute solution and blue-green to yellow light (470−563 nm) in the solid state. The photoluminescence emission was well-described by single-exponential decay with lifetimes ranging from 200 ps to 2.2 ns in both dilute solution and thin film, indicating lack of intermolecular emissive species in the solid state. PPV derivatives with quinoxaline moieties in the main chain (**QXPV1** and **QXPV2**) showed facile reversible electrochemical reductions with electron affinities of 2.63−2.75 eV. As emissive materials in LEDs, greenish-yellow electroluminescence with a brightness of up to 450 cd/m^2 was obtained from single-layer diodes of **QXPV1** with aluminum cathode in air.

Introduction

Organic light-emitting diodes (OLEDs) based on conjugated polymers such as poly(*p*-phenylenevinylene) (PPV) and polyfluorene have attracted much attention in the past decade as promising candidates for the next generation of full-color, flat-panel displays.[1−7] One of the many important challenges that still remain is the improvement of the external quantum efficiency (EQE) of OLEDs. Electroluminescence (EL) from OLEDs arises from the radiative decay of excitons generated by the recombination of electrons and holes injected from two opposite electrodes into the emissive polymer layer. Balanced rates of injection and transport of both electrons and holes are essential to achieving high EQE in an OLED. However, most emissive conjugated polymers such as PPVs have much higher hole mobility than electron mobility and low electron affinities, causing an imbalance in charge injection and transport and thus poor EQEs from single-layer OLEDs.[1−7] Several approaches have been explored to improve the device performance with varying degrees of success, including the use of low work function cathodes such as calcium (Ca) to improve electron injection and the utilization of a separate electron-transport (n-type) material in multilayers or blends with an emissive p-type polymer.[1−7]

One promising approach to improving the external quantum efficiency of OLEDs is to incorporate the functions of hole and electron transport and light emission into a single polymer, thereby creating bipolar (donor/acceptor) emissive polymers.[8−16] Rational molecular design of emissive polymers with improved electron affinity and balanced charge transport would allow the fabrication of efficient single-layer OLEDs. One of the challenges of this approach is to improve the charge transport properties while preserving the desired high luminescence quantum yields. Toward this end, several copolymers have been synthesized based on p-type backbones incorporating an electron-deficient unit such as pyridine,[8] cyano group,[9] oxadiazole,[10,11] quinoline,[12] or quinoxalines,[12−16] either in the main chain or as pendants to the main chain. Quinoxaline is a useful n-type building block with high electron affinity and good thermal stability. It has been successfully incorporated in small molecules and polymers for use as electron-transport materials in multilayer OLEDs based on PPV.[17−20] In contrast to the vast literature on oxadiazole-containing donor/acceptor copolymers, there are only a few reports on quinoxaline-containing copolymers based on p-type emissive backbones such as polyfluorene,[12,13] PPV,[14,15] and polycarbazole.[16] To the best of our knowledge, quinoxaline-containing PPVs have not yet been explored as emissive materials for OLEDs.

In this paper, we report the synthesis and characterization of four new PPV derivatives with one or two quinoxaline moieties incorporated either directly in the polymer backbone or as pendants to the main chain. Four dibromo-substituted quinoxalines, namely 2,3-bis(4-bromophenyl)quinoxaline,2,2′-bis(4-bromophenyl)-3,3′-diphenyl-6,6′-biquinoxalinyl, 2-(2,5-dibromophenyl)-3-phenylquinoxaline, and 2,2′-(2,5-dibromo-1,4-phenylene)bis(3-phenylquinoxaline), were synthesized and polymerized via Heck coupling. Systematic variation in the molecular structure of the copolymers via attachment of quinoxaline units at selective positions on the polymer backbone allows for detailed study of structure−property relationships. The photophysical properties of the copolymers in dilute solution and thin film and their electrochemical properties were investigated. The copolymers were used as both emissive and electron-transport materials in OLEDs.

* Corresponding authors. E-mail: makspil@upatras.gr; jenekhe@u.washington.edu.

10.1021/ma048903q CCC: $27.50
Published on Web 09/16/2004

Experimental Section

Characterization Methods. Melting temperatures were determined on an electrothermal melting point apparatus IA6304 and are uncorrected. IR spectra were recorded on a Perkin-Elmer 16PC FT-IR spectrometer with KBr pellets. ^{1}H NMR (400 MHz) and ^{13}C NMR (100 MHz) spectra were obtained using a Bruker spectrometer. The NMR spectra were recorded using DMSO-d_6 or $CDCl_3$ as solvent. Chemical shifts (δ values) are given in parts per million with tetramethylsilane as an internal standard. UV−vis absorption spectra were recorded on a Perkin-Elmer model Lambda 900 UV/vis/near-IR spectrophotometer. The photoluminescence (PL) emission spectra were obtained with a Photon Technology International (PTI) Inc. model QM-2001-4 spectrofluorimeter. GPC analysis was conducted on a Waters Breeze 1515 liquid chromatograph equipped with a 2410 differential refractometer as detector (Waters Associate) and Styragel HR columns using polystyrene as standard and THF as eluent. Differential scanning calorimetry (DSC) and thermogravimetric analysis (TGA) were performed on a DuPont 990 thermal analyzer system. Ground polymer samples of about 10 mg each were examined by TGA, and the weight loss comparisons were made between comparable specimens. The DSC thermograms were obtained at a heating rate of 10 °C/min in a N_2 atmosphere at a flow rate of 60 cm^3/min. Dynamic TGA measurements were made at a heating rate of 20 °C/min in atmospheres of N_2 or air at a flow rate of 60 cm^3/min. Thermomechanical analysis (TMA) was recorded on a DuPont 943 TMA using a loaded penetration probe at a scan rate of 10 °C/min in N_2 with a flow rate of 60 cm^3/min. The TMA experiments were conducted at least in duplicate to ensure the accuracy of the results. The TMA specimens were pellets of 8 mm diameter and 2 mm thickness prepared by pressing powder of polymer for 3 min under 5−7 kpsi at ambient temperature. Elemental analyses were carried out with a Hewlett-Packard model 185 analyzer.

To measure the PL quantum yields (Φ_f), polymer solutions in spectral grade chloroform were prepared. The concentration ($\sim 10^{-5}$ M) was adjusted so that the absorbance of the solution would be lower than 0.1. A 10^{-5} M solution of 9,10-diphenylanthracene in toluene ($\Phi_f = 0.93$) was used as a standard.[21] Cyclic voltammetry of the polymers was performed in acetonitrile with 0.1 M tetrabutylammonium hexafluorophosphate ($TBAPF_6$) as the supporting electrolyte at scan rates of 20−100 mV/s. Platinum wire electrodes were used as both counter and working electrodes, and silver/silver ion (Ag in 0.1 M $AgNO_3$ solution, from Bioanalytical Systems, Inc.) was used as a reference electrode. Using ferrocene as an internal standard, the potential values obtained were converted to vs SCE (saturated calomel electrode) and the corresponding ionization potential (IP) and electron affinity (EA) values were estimated from the onset redox potentials.

Time-Resolved PL Decay Dynamics. Fluorescence decays of the polymers in solution and thin film were measured on a PTI model QM-2001-4 spectrofluorimeter equipped with a Strobe Lifetime upgrade. The instrument utilizes a nanosecond flash lamp filled with high purity nitrogen/helium (30/70) mixture as an excitation source and a stroboscopic detection system. All measurements were done at room temperature. The decay curves were analyzed using a multiexponential fitting software package provided by the manufacturer. Reduced chi-square values, Durbin−Watson parameters, and weighted residuals were used as the goodness-of-fit criteria.

Fabrication and Characterization of LEDs. The single-layer OLEDs were fabricated as sandwich structures between aluminum (Al) cathodes and indium−tin oxide (ITO) anodes. ITO-coated glass substrates (Delta Technologies Ltd., Stillwater, MN) were cleaned sequentially in ultrasonic bathes of detergent, 2-propanol/deionized water (1:1 volume) mixture, toluene, deionized water, and acetone. A 50 nm thick hole injection layer of poly(ethylenedioxythiophene) doped with poly(styrenesulfonate) (PEDOT) was spin-coated on top of ITO from a 0.7 wt % dispersion in water and dried at 150 °C for 1 h under a vacuum. The copolymer solutions in chloroform were made at concentrations of 10−15 mg/mL and then filtered through 0.2 μm syringe filters. Thin films of copolymers and their 5 wt % blends with 1,1-bis(di-4-tolylaminophenyl)-cyclohexane (TAPC) were spin-coated from these solutions onto the PEDOT layer and dried at 50 °C in a vacuum overnight. The film thicknesses obtained were ca. 40−50 nm which were measured by an Alpha-Step 500 surface profiler (KLA Tencor, Mountain View, CA). Finally, 130−150 nm Al electrodes were thermally evaporated through a shadow mask onto the polymer films using an AUTO 306 vacuum coater (BOC Edwards, Wilmington, MA), typical evaporations being done at base pressures lower than 2×10^{-6} Torr. The active area of each EL device was 0.2 cm^2. For the bilayer OLEDs with PPV, a 60 nm film of PPV was spin-coated directly on top of ITO from its 0.6 wt % sulfonium precursor solution in water and cured at 220 °C for 100 min under a vacuum. Thin films ($\sim$25 nm) of the quinoxaline copolymers were spin-coated on top of the PPV layer from chloroform solutions and dried as aforementioned. Electroluminescence (EL) spectra were obtained using a PTI QM-2001-4 spectrophotometer. Current−voltage characteristics of the LEDs were measured using a HP4155A semiconductor parameter analyzer (Yokogawa Hewlett-Packard, Tokyo). The luminance was simultaneously measured using a model 370 optometer (UDT instruments, Baltimore, MD) equipped with a calibrated luminance sensor head (model 211). The device external quantum efficiencies were calculated using procedures reported previously.[11,22] All the device fabrication and characterization steps were done under ambient laboratory conditions.

Reagents and Solvents. Dimethylacetamide (DMAc) and tetrahydrofuran (THF) were dried by distillation over CaH_2. Chloroform and triethylamine were dried by distillation over P_2O_5 and KOH, respectively. 4,4′-Dibromobenzil and 1,2-phenelynediamine were recrystallized from 1,4-dioxane and toluene, respectively. 2,5-Didodecyloxy-1,4-divinylbenzene[9a] and 1,4-diiodo-2,5-dibromobenzene[23] were synthesized according to known methods. All other reagents and solvents were commercially purchased and were used as supplied.

Synthesis of Monomers (Schemes 1 and 2). 2,3-Bis(4-bromophenyl)quinoxaline (1). A solution of 4,4′-dibromobenzil (0.81 g, 2.20 mmol), 1,2-phenylenediamine (0.24 g, 2.20 mmol), and *p*-toluenesulfonic acid (23 mg) in $CHCl_3$ (15 mL) was refluxed under N_2 for 48 h. The solution was cooled to room temperature and filtered. The solvent was subsequently evaporated under reduced pressure, and the residue was recrystallized from acetonitrile to afford compound **1** (0.60 g, 62%) as a yellowish solid; mp 191−193 °C (lit.[24] 201−203 °C). Anal. Calcd for $C_{20}H_{12}N_2Br_2$: C, 54.58; H, 2.75; N, 6.36. Found: C, 54.31; H, 2.77; N, 6.33. FT-IR (KBr, cm^{-1}): 1586, 1556, 1448, 1390,1342, 1220, 1070, 1010, 976. ^{1}H NMR ($CDCl_3$, ppm): 8.30−8.28 (m, 2H, at positions 5 and 8 of quinoxaline); 7.95−7.92 (m, 2H, at positions 6 and 7 of quinoxaline); 7.65−7.63 (d, 4H, ortho to bromo); 7.55−7.53 (d, 4H, meta to bromo). ^{13}C NMR ($CDCl_3$, ppm): 152.31, 141.,67, 138.12, 132.08, 131.83, 130.78, 129.61, 124.10.

1-Bromo-4-(phenylethenyl)benzene (2). 4-Bromoiodobenzene (1.00 g, 3.53 mmol), $Pd(PPh_3)_2Cl_2$ (0.1240 g, 0.177 mmol), and CuI (0.0673 g, 0.353 mmol) were dissolved in THF (20 mL), and triethylamine (10 mL) was added under nitrogen. Phenylacetylene (0.36 g, 3.53 mmol) was added, and the mixture was stirred at room temperature for 24 h. Then it was filtered, and the volatile components were stripped off under reduced pressure. The residue was purified by column chromatography with CH_2Cl_2/*n*-hexane (1/1 v/v) as eluent to afford **2** as a yellow solid (0.70 g, 77%); mp 86−88 °C (lit.[25] 87−88 °C). FT-IR (KBr, cm^{-1}): 1488, 1442, 1392, 1068, 1008. ^{1}H NMR ($CDCl_3$, ppm): 7.46−7.40 (m, 4H, ortho and meta to bromo); 7.33−7.27 (m, 5H, other aromatic). ^{13}C NMR ($CDCl_3$, ppm): 133.44, 132.92, 132.01, 128.93, 128.82, 123.32, 122.88, 122.66.

4-Bromobenzil (3). To a solution of **2** (0.53 g, 2.06 mmol) in CH_2Cl_2 (10 mL), $KMnO_4$ (1.03 g, 6.50 mmol), $NaHCO_3$ (0.21 g, 2.50 mmol), and tetraethylammonium bromide (0.2 g) were added by dissolving in water (10 mL), and the mixture was rapidly stirred at room temperature for 48 h. The excess $KMnO_4$ was destroyed by addition of HCl and Na_2SO_3 until the red color disappeared. The organic layer was separated,

Scheme 1

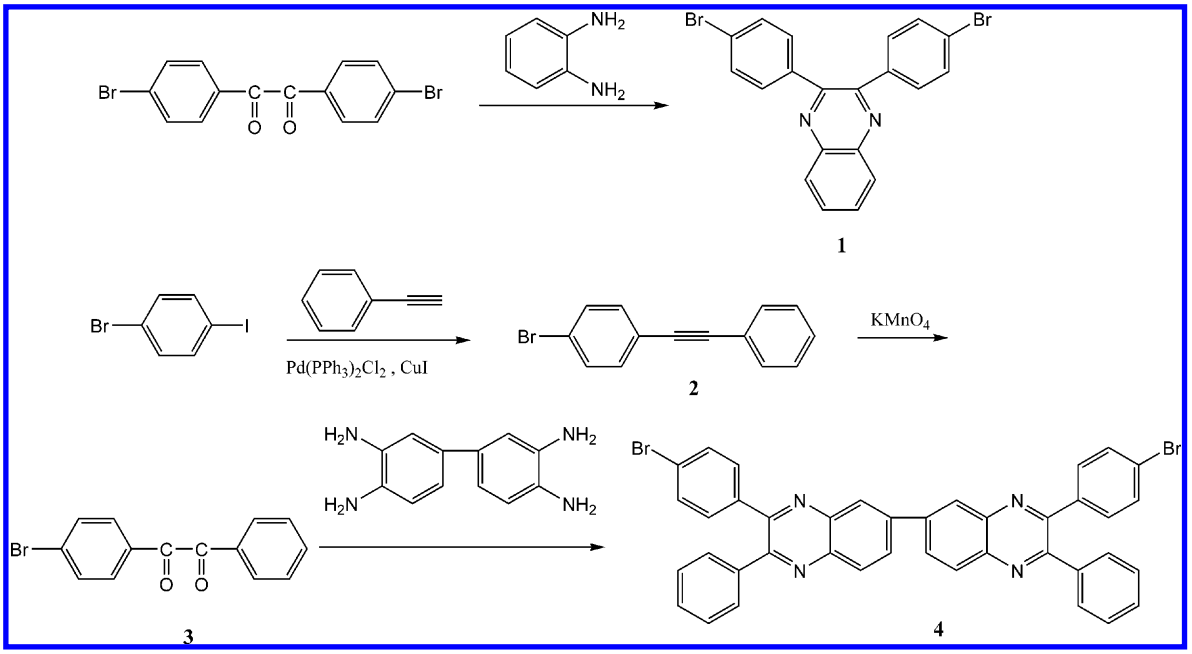

Scheme 2

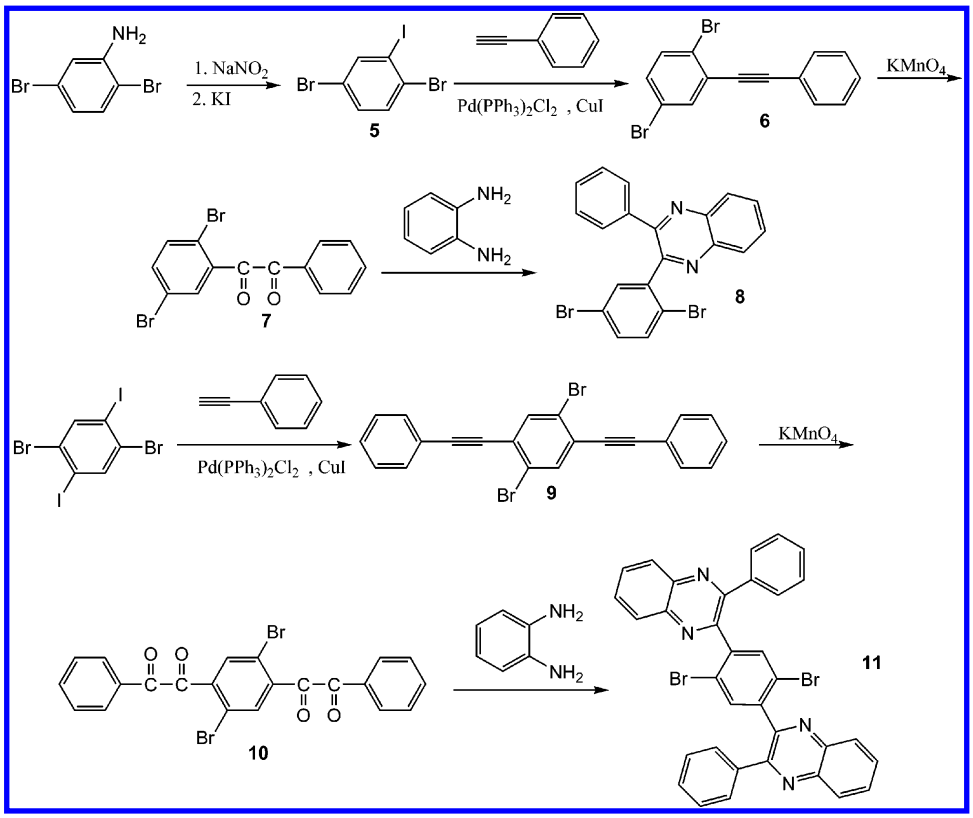

washed with sodium dicarbonate and water, and dried ($MgSO_4$). Evaporation of the solvent afforded compound **3** (0.58 g, 97%). It was recrystallized from methanol; mp 88−89 °C (lit.[26] 89−90 °C). FT-IR (KBr, cm^{-1}): 1668, 1582, 1210, 1174, 1070, 1010. ^1H NMR ($CDCl_3$, ppm): 7.97−7.95 (d, 2H, at positions 2′ and 6′); 7.85−7.84 (d, 2H, at positions 2 and 6); 7.69−7.65 (m, 3H, at positions 3′, 4′, and 5′); 7.54−7.51 (d, 2H, at positions 3 and 5). ^{13}C NMR ($CDCl_3$, ppm): 194.10, 193.53, 135.30, 133.34, 132.80, 132.30, 131.57, 130.77, 130.28, 129.41.

2,2′-Bis(4-bromophenyl)-3,3′-diphenyl-6,6′-biquinoxalinyl (4). Compound **4** was prepared (63%) as a yellow solid from the condensation of **3** with 3,3′-diaminobenzidine according to the procedure described for **1**. It was recrystallized from a mixture of methanol/1,4-dioxane; mp >300 °C. Anal. Calcd for $C_{40}H_{24}N_4Br_2$: C, 66.68; H, 3.36; N, 7.78. Found: C, 66.14; H, 3.32; N, 7.76. FT-IR (KBr, cm^{-1}): 1614, 1588, 1476, 1342, 1072, 1054, 1010, 978. ^1H NMR ($CDCl_3$, ppm): 8.60 (s, 2H, at positions 5, 5′); 8.32−8.23 (m, 4H, at positions 7, 7′, 8, 8′); 7.61−7.39 (m, 18H, other aromatic). ^{13}C NMR ($CDCl_3$, ppm): 141.84, 141.73, 141.43, 141.35, 139.12, 138.28, 131.91, 130.35, 130.22, 130.09, 130.04, 129.56, 128.92, 127.87.

2,5-Dibromoiodobenzene (5). To a solution of 2,5-dibromoaniline (2.60 g, 10.4 mmol) in glacial acetic acid (5 mL), 96% H_2SO_4 (2 mL) was added. The mixture was cooled to 0 °C, and a solution of $NaNO_2$ (2.14 g, 31.0 mmol) in water (5 mL) was added dropwise. After 1 h of stirring at 0 °C, urea

(1.2 g) in H_2O (4 mL) was added dropwise to destroy the excess of $NaNO_2$. Aqueous KI (5.16 g, 31.1 mmol) was added dropwise at room temperature, and the mixture was stirred at room temperature for 1 h. The brown precipitate was filtered, washed with water, and dried. It was purified by column chromatography with *n*-hexane as eluent affording compound **5** (2.60 g, 69%) as a white solid; mp 38−39 °C. FT-IR (KBr, cm^{-1}): 1544, 1436, 1352, 1246, 1096, 1078, 1002, 868, 810, 742, 516. ^1H NMR ($CDCl_3$, ppm): 7.99 (s, 1H, ortho to I); 7.47−7.45 (d, 1H); 7.33−7.31 (d, 1H). ^{13}C NMR ($CDCl_3$, ppm): 142.64, 133.92, 132.96, 129.03, 121.58, 102.42.

Compounds **6**, **9** and **7**, **10** as well as **8**, **11** (Scheme 2) were synthesized according to the procedures described for the corresponding compounds **1**, **2**, and **3** (Scheme 1), respectively.

1,4-Dibromo-2-(phenylethynyl)benzene (6). It was purified by column chromatography using *n*-hexane/CH_2Cl_2 (3:1 v/v) as eluent. Compound **6** was obtained as a white solid in 97% yield; mp 55−57 °C. FT-IR (KBr, cm^{-1}): 3070, 2215, 1595, 1569, 1488, 1460, 1439, 1377, 1075, 1031, 876, 805, 745, 683, 565. ^1H NMR ($CDCl_3$, ppm): 7.68 (s, 1H, at position 3); 7.57−7.55 (d, 2H, ortho to the triple bond); 7.47−7.45 (d, 1H, at position 6); 7.37−7.35 (m, 1H at position 5 and 3H meta and para to triple bond). ^{13}C NMR ($CDCl_3$, ppm): 136.03, 134.07, 132.76, 132.18, 129.40, 128.83, 127.74, 124.68, 122.84, 121.02, 95.67, 87.15.

2,5-Dibromobenzil (7). Recrystallized from ethanol 95% (yield 57%); mp 126−128 °C. FT-IR (KBr, cm^{-1}): 3082, 1672, 1594, 1570, 1452, 1380, 1198, 1178, 12086, 1026. ^1H NMR ($CDCl_3$, ppm): 8.09−8.07 (d, 2H, at positions 2′ and 6′); 7.92 (s, 1H, at position 6); 7.71−7.67 (d,1H, at position 4); 7.58−7.54 (m, 3H, at positions 3′, 4′, 5′); 7.50−7.48 (d, 1H, at position 3). ^{13}C NMR ($CDCl_3$, ppm): 193.00, 191.02, 138.27, 137.46, 135.36, 135.13, 132.74, 130.83, 129.34, 122.43, 120.54.

2-(2,5-Dibromophenyl)-3-phenylquinoxaline (8). Purified by recrystallization from CH_3CN (yield 99%); mp 188−190 °C. Anal. Calcd for $C_{20}H_{12}N_2Br_2$: C, 54.58; H, 2.75; N, 6.36. Found: C, 54.21; H, 2.78; N, 6.35. FT-IR (KBr, cm^{-1}): 3058, 1560, 1542, 1474, 1444, 1400, 1376, 1334, 1214, 1086, 1066, 1024, 980. ^1H NMR ($CDCl_3$, ppm): 8.26−8.18 (m, 2H, at positions 6 and 9); 7.88−7.81 (m, 2H, at positions 7 and 8); 7.70 (s, 1H, at positions 6 of pendant dibromophenyl); 7.53−7.51 (d, 2H, at positions 3 and 4 of pendant dibromophenyl); 7.39−7.32 (m, 5H, of pendant phenyl). ^{13}C NMR ($CDCl_3$, ppm): 153.73, 152.28, 142.56, 142.31, 140.98, 138.39, 134.72, 133.67, 131.18, 130.69, 130.02, 129.83, 129.63, 128.61, 121.83.

1,4-Dibromo-2.5-bis(phenylethynyl)benzene (9). Recrystallized from CH_3CN; mp 145−147 °C. FT-IR (KBr, cm^{-1}): 3072, 1496, 1440, 1354, 1064, 1024. ^1H NMR ($CDCl_3$, ppm): 7.79 (s, 2H, ortho to Br); 7.59−7.57 (m, 4H, ortho to triple bonds); 7.39−7.37 (m, 6H, meta and para to triple bonds). ^{13}C NMR ($CDCl_3$, ppm): 136.44, 132.22, 129.54, 128.87, 126.84, 124.13, 122.74, 97.08, 87.22.

1,1′-(2,5-Dibromo-1,4-phenylene)bis(2-phenylethanedione) (10). Recrystallized from ethyl acetate; mp 205−207 °C. FT-IR (KBr, cm^{-1}): 3084, 1693, 1593, 1451, 1358, 1273, 1183, 1085. ^1H NMR (DMSO-d_6, ppm): 8.18 (s, 2H, ortho to Br); 8.12−810 (d, 4H, ortho to triple bond); 7.85−7.65 (m, 6H, meta and para to triple bond). ^{13}C NMR (DMSO-d_6, ppm): 192.00, 190.03, 141.48, 136.78, 135.40, 132.46, 130.92, 129.44, 120.81.

2,2′-(2,5-Dibromo-1,4-phenylene)bis(3-phenylquinoxaline) (11). Recrystallized from DMAc/H_2O (4/1); mp >300 °C. Anal. Calcd for $C_{34}H_{20}N_4Br_2$: C, 63.38; H, 3.13; N, 8.69. Found: C, 62.94; H, 3.10; N, 8.72. FT-IR (KBr, cm^{-1}): 3056, 1556, 1538, 1478, 1442, 1396, 1358, 1210, 1088, 1048, 1028. ^1H NMR (DMSO-d_6, ppm): 8.24−8.18 (m, 4H, at positions 5 and 8 of quinoxaline); 7.88−7.82 (m, 4H, at positions 6 and 7 of quinoxaline); 7.65 (s, 2H, ortho to Br); 7.50−7.30 (m, 10H, of pendant phenyls).

Synthesis of Polymers. Polymer QXPV1. The preparation of polymer **QXPV1** is given as a typical example. A round-bottom flask equipped with magnetic stirrer, reflux condenser, and gas input−output was charged with a mixture of **1** (0.57 g, 1.30 mmol), 1,4-didocyloxy-2,5-divinylbenzene (0.65 g, 1.30 mmol), $Pd(OAc)_2$ (0.0120 g, 0.054 mmol), and tri-*o*-tolylphosphine (0.0910 g, 0.299 mmol). The flask was evacuated and purged with argon. DMAc (15 mL) and triethylamine (5 mL) were added with a syringe, and the mixture was heated at 120 °C for 36 h. After cooling to room temperature, the solution was filtered and the filtrate was poured in methanol. The yellow precipitate was filtered, washed with methanol, and dried to afford polymer **QXPV1** (0.87 g, 87%). The polymer was purified by dissolution in THF, filtration, and reprecipitation in methanol. M_n = 12 700; polydispersity (PDI) = 2.3 (by GPC). Anal. Calcd for $(C_{54}H_{68}N_2O_2)_n$: C, 83.46; H, 8.82; N, 3.60. Found: C, 82.55; H, 8.94; N, 3.53.

Polymer QXPV2. It was prepared in 82% yield from the polymerization of **4** with 1,4-didocyloxy-2,5-divinylbenzene. M_n = 15 600; PDI = 2.1 (by GPC). Anal. Calcd for $(C_{74}H_{80}N_4O_2)_n$: C, 84.05; H, 7.63; N, 5.30. Found: C, 83.24; H, 7.68; N, 5.26.

Polymer QXPV3. It was prepared from the polymerization of **8** with 1,4-didocyloxy-2,5-divinylbenzene in 74% yield. M_n = 8200; PDI = 1.8 (by GPC). Anal. Calcd for $(C_{54}H_{68}N_2O_2)_n$: C, 83.46; H, 8.82; N, 3.60. Found: C, 82.52; H, 8.71; N, 3.55.

Polymer QXPV4. It was prepared according to the aforementioned method from the reaction of **11** with 1,4-didodecyloxy-2,5-divinylbenzene in 88% yield. M_n = 14 500; PDI = 2.6 (by GPC). Anal. Calcd for $(C_{68}H_{76}N_4O_2)_n$: C, 83.22; H, 7.81; N, 5.71. Found: C, 82.31; H, 7.78; N, 5. 77.

Results and Discussion

Synthesis and Characterization. Schemes 1 and 2 show the synthesis of dibromides **1**, **4**, **8**, and **10**. Compound **1** was easily prepared from commercially available 4,4′-dibromobenzil. The other dibromides were successfully prepared via multistep procedures. The first substantial step of the procedure was the synthesis of bromo-substituted (phenylethynyl)benzenes **2**, **6**, and **9** that were prepared from Sonogashira coupling of 4-bromoiodobenzene with phenylacetylene. Their synthesis was based on the higher reactivity iodobenzene relative to bromobenzene toward Sonogashira coupling. As a result, the bromoiodobenzenes were exclusively alkynylated through the iodo group at ambient temperature.[27] The second step of the procedure involved the oxidation of the triple bond to diketones **3**, **7**, and **10**.[28] Finally, the condensation of the latter as well as of the commercially purchased 4,4′-dibromobenzil with 1,2-phenylenediamine or 3,3′-diaminobenzidine afforded dibromoquinoxalines **1**, **4**, **8**, and **11**.

Polymers **QXPV1**, **QXPV2**, **QXPV3**, and **QXPV4** (Chart 1) were prepared from dibromides **1**, **4**, **8**, and **11**, respectively, and 1,4-didodecyloxy-2,5-divinylbenzene via Heck coupling. They were obtained in 74−88% yields, and their number-average molecular weights (M_n) ranged from 8200 to 15 600 with polydispersity indices (PDI) of 1.8−2.6 (Table 1). The polymers had molecular weights comparable to those of other polymers obtained through Heck coupling.[8a,9a,11] The structures of the polymers were verified by FT-IR, ^1H NMR spectroscopy, and elemental analysis. The FT-IR spectra of the polymers displayed absorption features that are consistent with their structures, at about 2924, 2850 (aliphatic), 1620−1460 (aromatic), 1210 (ether bonds), and 970 cm^{-1} (trans olefinic bonds). The ^1H NMR spectra of all the polymers exhibited peaks at about 8.60−7.00 (aromatic and olefinic protons), 4.00 (O−CH_2−), and 1.80−0.81 ppm (−$(CH_2)_{10}$−CH_3). The peaks of olefinic protons resonated at 7.20−7.00 ppm, supporting the formation of trans olefinic bond. In addition, no peak was observed at 6.5−5.5 ppm, indicating the absence of cis olefinic bond and terminal vinyl groups. Figure 1 shows the ^1H NMR spectrum of polymer **QXPV1** as a typical example, and Figure 2 shows the ^{13}C NMR of polymer **QXPV3**.

Chart 1

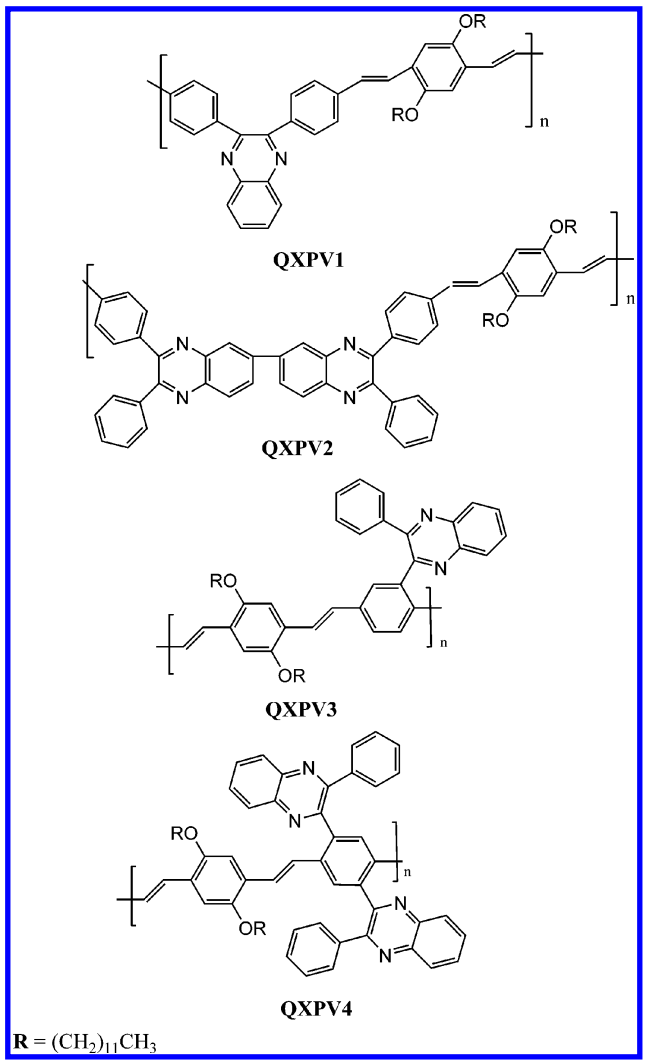

Table 1. Molecular Weights and Thermal Properties of Polymers

polymer	M_n[a]	M_w/M_n[a]	T_g[b] (°C)	T_m[c] (°C)	T_d[d] (°C)	Y_c[e] (%)
QXPV1	12 700	2.3	n.o.[f]	70	355	30
QXPV2	15 600	2.1	140	n.o.	370	52
QXPV3	8 200	1.8	n.o.	90	340	41
QXPV4	14 500	2.6	155	n.o.	380	60

[a] Molecular weights were determined by GPC using polystyrene standards. [b] Glass transition temperature. [c] Melting temperature. [d] Decomposition temperature in nitrogen (at which 1% weight loss was observed). [e] Anaerobic char yield at 800 °C. [f] n.o. = not observed.

Qualitative studies demonstrated that the polymers were soluble in common organic solvents such as THF, $CHCl_3$, CH_2Cl_2, 1,2-dichloroethane, 1,1,2,2-tetrachloroethane, chlorobenzene, and toluene due to the long dodecyloxy side chains. In addition, they were slightly soluble in trifluoroacetic acid and partially soluble in formic acid due to the protonation of the quinoxaline rings. Polymers **QXPV1** and **QXPV3**, which contain one quinoxaline ring per repeat unit, exhibited higher solubility than **QXPV2** and **QXPV4**, which carry two quinoxaline rings per repeat unit. In addition, the polymers that bear quinoxaline moieties in the main chain were more soluble than the polymers with pendant quinoxalines units. **QXPV4** was the least soluble polymer due to the two bulky pendant quinoxaline groups with a maximum solubility of only about 3 mg/mL in THF or chloroform. The poor solubility made it difficult to spin-coat uniform thick films of **QXPV4** for making LEDs; however, thin films for photophysical studies could be solvent cast on glass substrates.

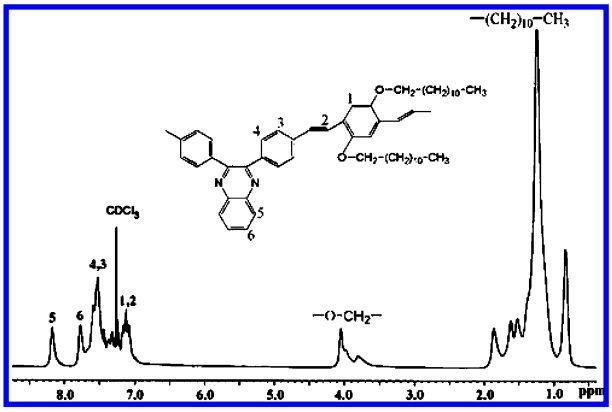

Figure 1. ^{1}H NMR spectrum of polymer **QXPV1** in $CDCl_3$.

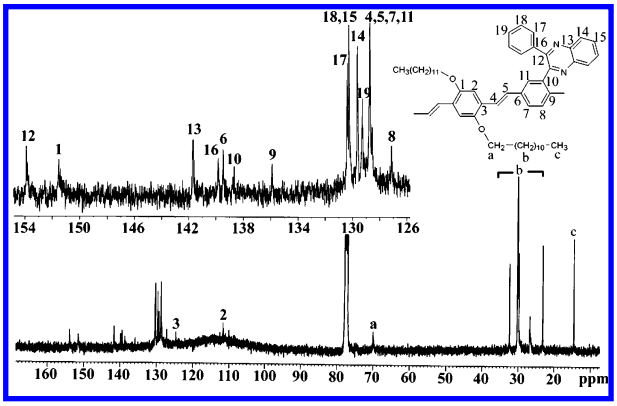

Figure 2. ^{13}C NMR spectrum of polymer **QXPV3** in $CDCl_3$.

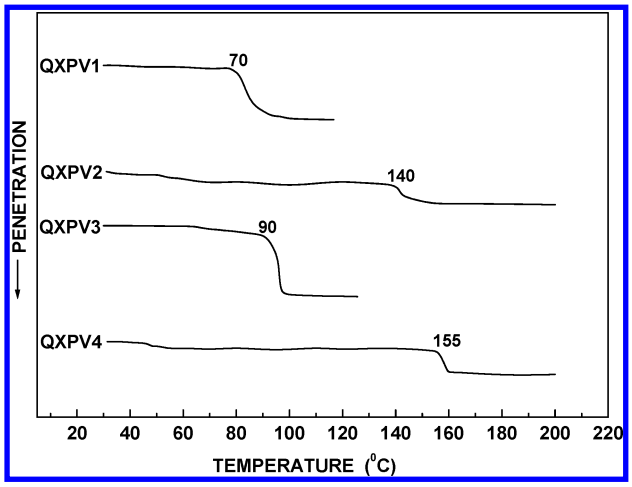

Figure 3. TMA traces of the polymers.

The thermal behavior of the polymers was investigated by DSC and TMA, and their thermal stability was evaluated by TGA. Figure 3 shows the TMA traces of the four polymers. Polymers **QXPV1** and **QXPV3**, bearing one quinoxaline moiety per repeat unit, exhibited melting transition (T_m) at 70 and 90 °C, respectively. This transition was detected by both DSC and TMA. Polarized microscopy showed that these polymers turn into an isotropic melt and confirmed the absence of thermotropic behavior. Compared to analogous dialkoxy-substituted PPVs, the T_m of the present polymers is lowered by more than 60 °C with incorporation of the quinoxaline moieties.[29a] No T_gs were observed for poly-

mers **QXPV1** and **QXPV3** by DSC or TMA. However, polymers **QXPV2** and **QXPV4** carrying two quinoxaline groups per repeat unit showed clear T_g at 140 and 155 °C, respectively. These T_gs were determined by the TMA method utilizing a loaded penetration probe as the onset temperature of the first inflection point of the corresponding TMA traces (Figure 3). The T_gs of the present polymers are more than 100 °C higher than those of analogous dialkoxy-substituted PPVs.[29a] The absence of melting and the high T_g of **QXPV2** and **QXPV4** reflect their higher rigidity due to the presence of two quinoxaline moieties per repeat unit. Similar enhancements of T_g were observed for polyfluorenes with the incorporation of the quinoxaline units in their main chains.[12a] Wide-angle X-ray diffractograms of the "as-prepared" powder of polymers revealed that **QXPV1** possessed a certain degree of crystallinity whereas **QXPV2** was completely amorphous. Besides, **QXPV2** and **QXPV4** exhibited a transition at about 50 °C, which was attributed to side chain melting in accordance with previous didodecyloxy-substituted PPVs.[29a] All the polymers showed satisfactory thermal stability, being stable up to 340−380 °C under nitrogen. Polymers containing two quinoxaline moieties per repeat unit (**QXPV2** and **QXPV4**) were relatively more stable than those with one quinoxaline per repeat unit (**QXPV1** and **QXPV3**) due to the excellent thermal stability characteristics inherent to the quinoxaline group. The anaerobic char yields of the polymers at 800 °C ranged from 30 to 60%. The thermal properties of the polymers are collected in Table 1.

Photophysical Properties. The optical absorption and photoluminescence (PL) emission spectra of the four polymers in dilute (10^{-5} M) chloroform solution are shown in Figure 4, parts a and b. All polymers except **QXPV4** showed a broad low-energy absorption band around 400 nm, typical of the $\pi-\pi^*$ transition of the conjugated PPV backbone.[29] Polymer **QXPV1** with one quinoxaline unit in the backbone showed an absorption peak at 402 nm, whereas polymer **QXPV3** with one pendant quinoxaline unit had the maximum located at 420 nm. **QXPV1** had a higher absorption onset than **QXPV3**, suggesting a smaller conjugation length in **QXPV1**. This can be explained by the greater interruption in conjugation caused by the presence of the quinoxaline unit in the PPV backbone in **QXPV1** vs pendant substitution in **QXPV3**. Polymer **QXPV2** with two quinoxaline units in the backbone had a higher absorption maximum at 388 nm, while **QXPV4** had the most blue-shifted peak at 354 nm with a significantly higher absorption onset at ∼390 nm. This suggests a drastic reduction in electron delocalization in **QXPV4** caused by substantial twisting of the backbone by the two bulky pendant quinoxaline units, given that polymer chains in dilute solution possess a high degree of rotational freedom. The high-energy absorption peak at ∼350 nm was observed only in polymers **QXPV3** and **QXPV4** with pendant substitution of quinoxalines, suggesting that it could be associated with the aromatic quinoxaline moieties rather than the PPV backbone. Overall, we note that the absorption features in all four polymers are blue-shifted compared to typical dialkoxy-substituted PPVs,[29] indicating that the conjugation length is decreased by inserting the quinoxaline moieties either in the main chain or as pendants.

It is known that the electronic character of a substituent influences the optical properties of the polymers. The introduction of an electron-donating or -accepting group directly affects the HOMO and LUMO levels of the polymer. In our case, the insertion of the electron-withdrawing quinoxalines on a PPV backbone changed drastically its properties. The introduction of one quinoxaline moiety caused a blue shift of the UV−vis spectra of polymers relative to alkoxy-PPV. This shift was larger in the case of **QXPV1**, which contains the quinoxaline unit in the main chain, than **QXPV3**, where the quinoxaline is laterally attached to the polymer backbone. This might be due to the direct participation of quinoxaline in the $\pi-\pi^*$ transition of the main chain of polymer **QXPV1**. In the case of **QXPV3**, a reasonable noncoplanar assembly of quinoxaline side group and the polymer backbone may reduce the effects of quinoxaline unit on polymer, hence a smaller blue shift of the UV−vis spectrum than that of **QXPV1**. The introduction of a second quinoxaline group either in the main chain or as a side group brought about an additional blue shift of absorption and emission of the polymer **QXPV2** and **QXPV4**, respectively. It is believed that it is a result of steric effects due to insertion of the second bulk substituent rather than their effect on electronic properties of the polymers. More insight into the effects of quinoxalines moieties on the polymers properties appears in the Electrochemical Properties section.

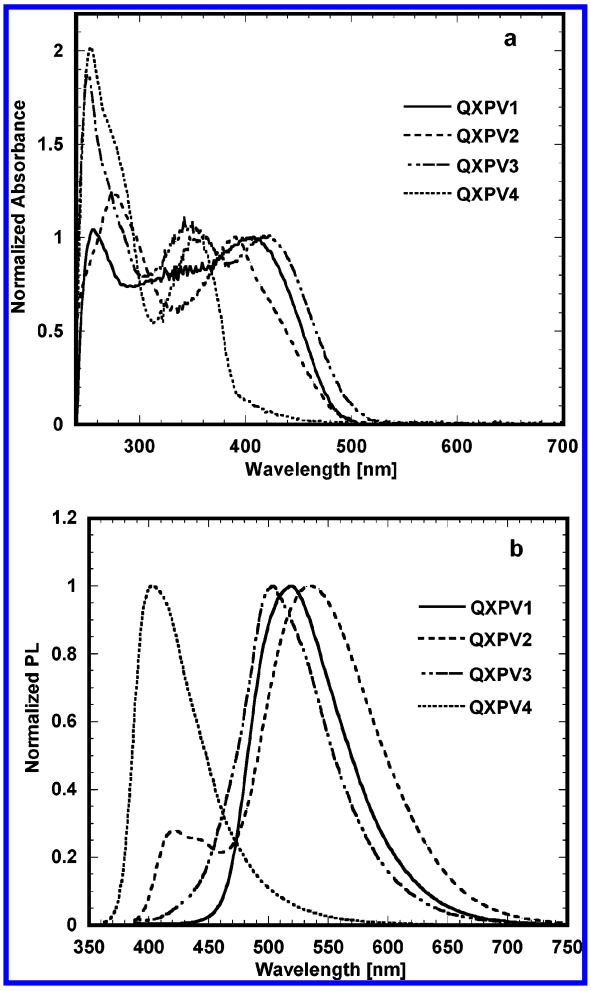

Figure 4. (a) Normalized optical absorption spectra of 10^{-6} M solutions of the four copolymers in chloroform. (b) Normalized PL emission spectra of 10^{-6} M solutions of the copolymers in chloroform. Excitation wavelength is 380 nm in all cases except for **QXPV4** (360 nm).

Table 2. Photophysical Properties of Polymers

polymer	$\lambda_{a,max}$[a] in solution (nm)	$\lambda_{f,max}$[b] in solution (nm)	Φ_f[c]	$\lambda_{a,max}$[a] in thin film (nm)	$\lambda_{f,max}$[b] in thin film (nm)	E_g[d] (eV)
QXPV1	402	519	0.55	404	539	2.59
QXPV2	388	419, *536*	0.34	397	547	2.57
QXPV3	*348*,[e] 420	504	0.21	*350*, 425	563	2.38
QXPV4	354	404	0.19	355	470	3.05

[a] $\lambda_{a,max}$: the absorption maxima in chloroform solution or in thin film. [b] $\lambda_{f,max}$: the PL emission maxima in chloroform solution or in thin film. [c] Φ_f: PL quantum yield in chloroform solution. [d] E_g: optical band gap calculated from thin film absorption edge. [e] Italic numerical values denote absolute maxima.

Figure 4b shows the PL emission spectra of the four polymers in dilute chloroform solution. The excitation wavelength used is 380 nm in all cases except for polymer **QXPV4** (360 nm). Polymers **QXPV1** and **QXPV2** with quinoxalines in the main chain had emission maxima at 519 and 536 nm, respectively. However, **QXPV3** and **QXPV4** had blue-shifted emissions at 504 and 404 nm, respectively. One would have expected that **QXPV3** would have the most red-shifted emission due to its longer conjugation length. However, polymer **QXPV2** shows the lowest energy emission band at 536 nm. Since **QXPV2** has the long docecyloxy side chains spaced farthest apart per repeat unit due to two quinoxaline units, it is likely that there could be planarization of the backbone in the excited state leading to the bathochromic shift in its emission. The additional peak at 419 nm could be likely due to the exciton localization on the two neighboring quinoxaline units. It is rather surprising that the presence of an additional pendant quinoxaline unit in **QXPV4** compared to **QXPV3** blue shifts its emission maximum significantly by 100 nm. Compared to analogous dialkoxy-substituted PPVs,[29] the PL emission spectra of the present quinoxaline-containing PPVs are not only blue-shifted but also lack any well-resolved vibronic structure due to apparent lack of intrachain order. The main photophysical properties of the quinoxaline PPVs are summarized in Table 2.

The absorption spectra of thin films of the four quinoxaline PPVs are shown in Figure 5a. They are very similar to the dilute solution absorption spectra in terms of the spectral shapes and peak positions. The lowest energy transitions of polymers **QXPV1** and **QXPV3** were located at 404 and 425 nm, respectively. Polymers **QXPV2** and **QXPV4** with two quinoxalines per repeat unit showed blue-shifted transitions at 397 and 355 nm, respectively. The similarity of the thin film spectra to the dilute solution spectra suggests comparable ground-state electronic structures with minimal interchain aggregation even in the condensed state. The optical band gaps derived from the absorption edge of the thin film spectra gave similar values of 2.4−2.6 eV for all polymers except **QXPV4**, which had a higher band gap of ∼3.0 eV. Figure 5b shows the PL emission spectra of the polymer thin films with excitation being done at the low-energy absorption maximum of each polymer. The polymers emit greenish-yellow light in thin film, except **QXPV4** which emits greenish-blue color. The emission maxima of polymers **QXPV1** and **QXPV2** are red-shifted by 10−20 nm compared to their corresponding dilute solution spectra (Figure 4b). This can be explained as due to increased exciton delocalization in the thin films due to the interchain π-stacking. The red shift of ∼60−65 nm in the emission maxima of polymers **QXPV3** and **QXPV4** in going from dilute solution to the thin film state is much greater. Given that the rotational freedom of the polymer chains in the solid state is much

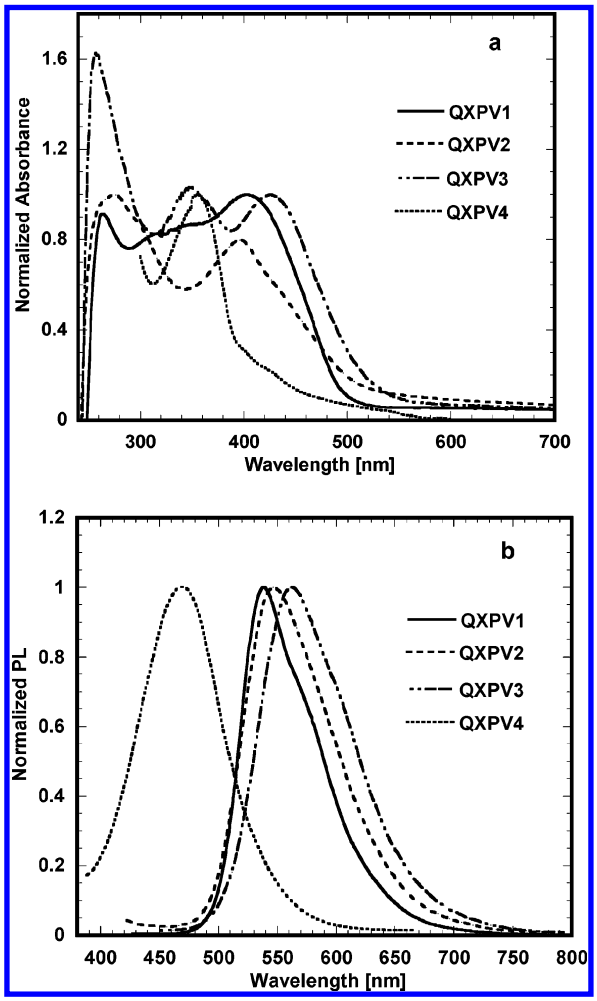

Figure 5. (a) Normalized optical absorption spectra of the four copolymer thin films. (b) Normalized PL emission spectra of the four copolymer thin films. In each case, the excitation wavelength is the absorption maximum in (a) above.

reduced, the pendant quinoxaline units could force the PPV backbones in **QXPV3** and **QXPV4** to adopt more planar conformations in the solid state than in solution, leading to the much red-shifted emission peaks at 563 and 470 nm, respectively. Besides, we observe a slight vibronic structure in the PL spectra of polymers **QXPV1** and **QXPV3**, reminiscent of the typical emission spectra of dialkoxy-substituted PPVs.[29] This could be due to some interchain ordering due to a certain degree of crystallinity in these two polymer films as evidenced by WAXD patterns (not shown).

The fluorescence quantum yields (ϕ_f) of the four polymers in dilute chloroform solution are listed in Table 2. The highest ϕ_f value of 55% was observed for polymer **QXPV1**, which is higher than that of MEH−PPV and comparable to CN−PPV.[30] Polymers **QXPV3** and **QXPV4** had the lowest ϕ_f values of ∼20%. The

Table 3. Fluorescence Decay Lifetimes of Polymer Solutions and Thin Films

polymer	λ_{exc}[a] (nm)	λ_{em}[b] (nm)	τ[c] (ns)	χ^2	DW[d]
solution					
QXPV1	381	519	1.637	1.106	1.716
QXPV2	381	536	2.201	1.08	1.816
QXPV3	381	504	1.611	1.072	1.541
QXPV4	358	404	1.55	1.08	2.04
thin film					
QXPV1	381	547	0.604	1.173	1.801
QXPV2	381	539	1.167	0.9267	1.947
QXPV3	381	563	0.197	0.9435	2.091

[a] Excitation wavelength. [b] Monitored emission wavelength. [c] Fluorescence lifetime extracted from the single-exponential fits. [d] Durbin−Watson parameter for the fits. Concentration of all solutions was 10^{-5} M in chloroform.

Table 4. Redox Potentials and Electronic Structure Parameters of Polymers

polymer	E_{onset}[a] oxidation (V)	E_{onset}[a] reduction (V)	IP (eV)[b]	EA (eV)[c]	E_g^{el} (eV)[d]
QXPV1	0.88	−1.77	5.28	2.63	2.65
QXPV2	0.87	−1.65	5.27	2.75	2.52
QXPV3	0.75	−1.75	5.15	2.65	2.50
QXPV4	0.90	−1.70	5.30	2.70	2.60

[a] E_{onset} = onset potential vs SCE. [b] Determined from the onset oxidation potential. [c] Determined from the onset reduction potential. [d] Electrochemical band gap = IP − EA.

polymers with quinoxaline pendant units seemed to have lower ϕ_f values than the ones with backbone substitution of quinoxalines. Thus, by subtle variations in the number and point of attachment of the quinoxaline moieties on the PPV backbones, we observed systematic variations in the steady-state photophysical properties of the four polymers.

Time-Resolved PL Decay Dynamics. To further shed light on the nature of the emission from the quinoxaline-containing polymers, we investigated the fluorescence decays of the polymer PL emission bands in solution and thin film. A summary of the fluorescence decay parameters is presented in Table 3. In dilute solution (10^{-5} M), the decay of the lowest energy emission band for all the polymers was found to be single-exponential with lifetimes ranging from 1.5 to 2.2 ns. This suggests that the emission originates from intrachain singlet excitons as would be expected for polymer chains with minimal interchain interactions. These lifetimes are longer than the typical lifetimes observed for other PPV-based polymers such as MEH−PPV and CN−PPV in dilute solution.[30] Knowledge of the fluorescence quantum yields in solution and the fluorescence lifetimes can give information on the natural radiative lifetimes (τ_0) of the emission bands. τ_0 values of 2.98 and 7.67 ns were obtained for the PL emission of **QXPV1** and **QXPV3**, respectively. The much smaller τ_0 value in **QXPV1** suggests a significantly faster radiative rate constant leading to the highest fluorescence yield observed among the four polymers.

In going from the polymer dilute solutions to thin films, the PL emission lifetimes decreased by more than 50%. However, the fact that the fluorescence was still well-described by single-exponential decay and that the steady-state PL spectra showed a slight vibronic structure ruled out any interchain related emissive species such as excimers in the thin films.[31] The fluorescence lifetimes of **QXPV1** (604 ps) and **QXPV2** (1.16 ns) are longer than those observed for thin films of PPV or MEH−PPV.[30] Although we did not measure the fluorescence quantum yields in thin films, visual observation of the films under excitation indicates higher quantum yields than PPV, with **QXPV1** being the most fluorescent. The drastic reduction in lifetime from 1.61 to 0.19 ns in going from solution to thin films of **QXPV3** suggests a greater number of channels for nonradiative decay of excitons. The greater conformational defects along the polymer backbone introduced by the bulky pendant quinoxaline units could be preferential sites for such nonradiative processes. We could not obtain good fluorescence decay curves for films of **QXPV4** due to the poor quality of the solvent cast films and their low fluorescence yields. The general approach of incorporating quinoxaline units in the main chain or as pendants seems to reduce the propensity to form interchain excitations and excimer-like emissions in thin films, unlike in CN−PPV thin films where efficient excimer emission is clearly observed.[30a] It is also interesting that relatively high PL emission quantum yields were observed in polymers **QXPV1** and **QXPV2** given that these copolymers have a donor/acceptor architecture. Strong intramolecular charge transfer in donor/acceptor conjugated polymers is usually a major source of dramatic luminescence quenching in such materials.[32] Our photophysical results imply that there is little or no contribution of intramolecular charge transfer to the photoexcitations of the donor/acceptor copolymers **QXPV1** and **QXPV2**.

Electrochemical Properties. To understand the variation in the electronic structure of the PPV derivatives by incorporation of the electron-deficient quinoxaline moieties, we performed cyclic voltammetry (CV) measurements on polymer films. The redox scans of polymers containing quinoxaline moieties in the main chain, **QXPV1** and **QXPV2**, are shown in Figure 6, parts a and b, respectively. Several reduction scans were taken at increasing scan rates ranging from 20 to 100 mV/s in steps of 20 mV. **QXPV1** showed a one-peak reversible reduction with a formal potential of −1.85 V vs SCE and an onset potential of −1.77 V vs SCE. However, the oxidation scan was completely irreversible with onset potential of +0.88 V vs SCE. Taking −4.4 eV as the SCE energy level relative to vacuum,[33] electron affinity (EA) and ionization potential (IP) energy levels of 2.63 and 5.28 eV were estimated. The presence of an additional quinoxaline moiety in the main chain in polymer **QXPV2** leads to the emergence of a second reversible reduction peak with a formal potential of −1.68 V vs SCE, in addition to the peak at −1.85 V seen in **QXPV1**. The reduction scans on both polymers are highly reversible with repeatable scans made on the same thin film samples without any changes in their peak characteristics. The onset reduction potential of −1.65 V leads to an EA value of 2.75 eV for **QXPV2**, which is slightly higher than that of **QXPV1** as would be expected with the additional quinoxaline moiety. Compared to the EA values of analogous dialkoxy-substituted PPVs such as MEH−PPV (EA = 2.9−3.0 eV), the EA values of the present polymers are slightly lower despite the presence of electron-deficient quinoxaline moieties in their backbones. Additionally, unlike in MEH−PPV, the oxidation scans of the current polymers are irreversible, suggesting that the ease of p-doping the PPV backbone is lost on introduction of the quinoxaline moieties.

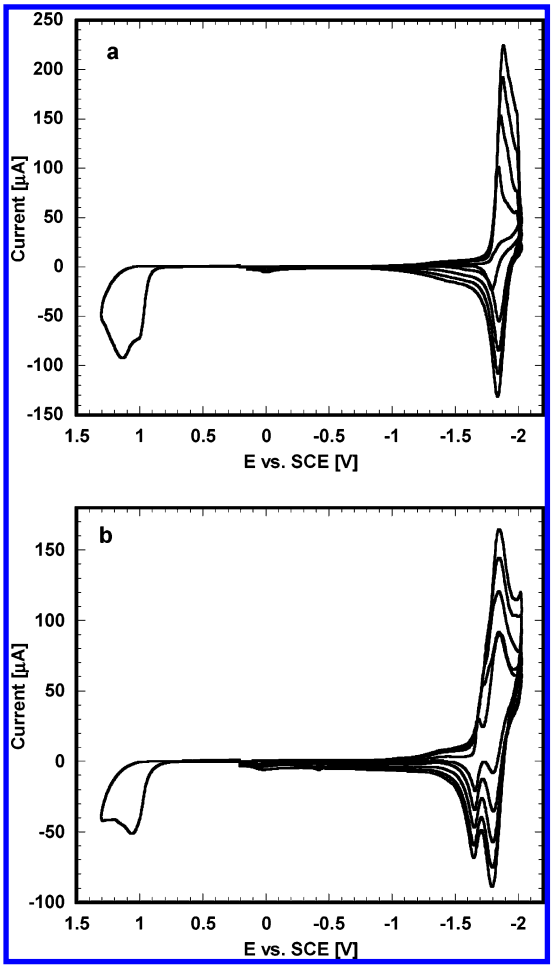

Figure 6. Cyclic voltammograms of (a) **QXPV1** and (b) **QXPV2** in 0.1 M $TBAPF_6$ in acetonitrile. The scan rates for the reduction waves range from 20 to 100 mV/s.

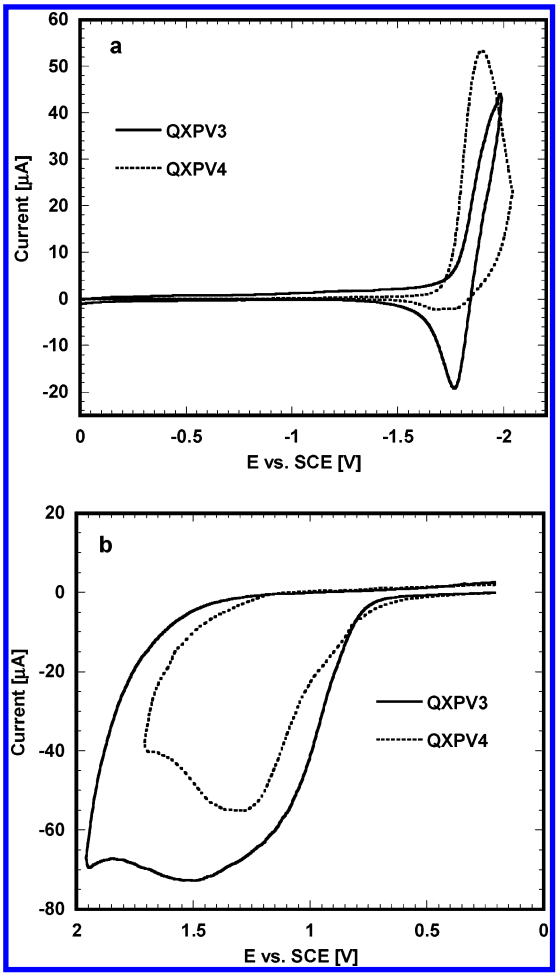

Figure 7. Cyclic voltammograms of **QXPV3** and **QXPV4** in 0.1 M $TBAPF_6$ in acetonitrile: (a) reduction waves and (b) oxidation waves. The scan rate used was 40 mV/s.

Figure 7, parts a and b, shows the reduction and oxidation waves at scan rates of 40 mV/s, respectively, of the polymers with pendant quinoxaline units **QXPV3** and **QXPV4**. We observed a reversible reduction and irreversible oxidation for **QXPV3** with one pendant quinoxaline unit. EA of 2.65 eV and IP of 5.15 eV were estimated from the onset redox potentials. However, the reduction waves were not as well-defined and repeatable as with polymers **QXPV1** and **QXPV2**. Similar characteristics were observed in the redox waves of **QXPV4** where complete reversibility in the reduction waves could not be captured due to dissolution of the doped polymer in the electrolyte after the first uptake of an electron. The poor characteristics of the redox waves of **QXPV4** could be in part due to the poor quality of the polymer thin films on the Pt electrodes. However, comparing Figures 6 and 7, it is evident that the polymers with quinoxaline moieties in the main chain (**QXPV1** and **QXPV2**) are more amenable to n-type doping than those with pendant quinoxaline units (**QXPV3** and **QXPV4**). One plausible reason for this trend could be the fact that the quinoxaline moieties in the main chain directly participate in the conjugation along the polymer backbone, whereas the pendant quinoxalines do not. In fact, the redox scans in Figure 6 are very reminiscent of typical n-type conjugated polymers such as the polyquinolines[3,4,6] and polybenzobisazoles.[7b] The incorporation of electron-deficient quinoxalines in the polymer backbones has apparently transformed the PPV-based polymers into n-type polymers, suggesting better electron-transport characteristics than hole transport. A similar transformation of PPV to n-type polymers was previously observed by incorporation of one or two oxadiazole moieties in the backbone of PPV-based polymers.[11] Thus, we do not realize true bipolar behavior in these donor−acceptor type quinoxaline PPVs, which has implications in relation to charge injection properties for light-emitting diodes (LEDs) based on these polymers as discussed next.

EL Device Properties. Light-emitting diodes (LEDs) based on the quinoxaline copolymers as both emissive and electron transport materials were made and investigated. Figure 8a shows the current density−voltage−luminance ($J-V-L$) characteristics of single-layer **QXPV1** LEDs of the type ITO/PEDOT/polymer/Al. Diodes comprising of neat polymer layer had a turn-on voltage of ca. 6 V with a maximum brightness of 120 cd/m^2 and maximum external quantum efficiency (EQE) of 0.012% at 12.5 V (115 cd/m^2, 260 mA/cm^2). The corresponding EL spectra shown in Figure 8b were similar to the thin film PL spectra with EL maxima centered at ∼535 nm. There was a slight blue shift from 535 nm (7.0 V) to 528 nm (13 V) with increase in applied bias. This suggests that the greater local heating in the polymer film at the high voltages probably leads to conformational changes of the polymer backbone, especially given that **QXPV1** has a melting transition at 70 °C (Table 1). Although the device performance of this simple

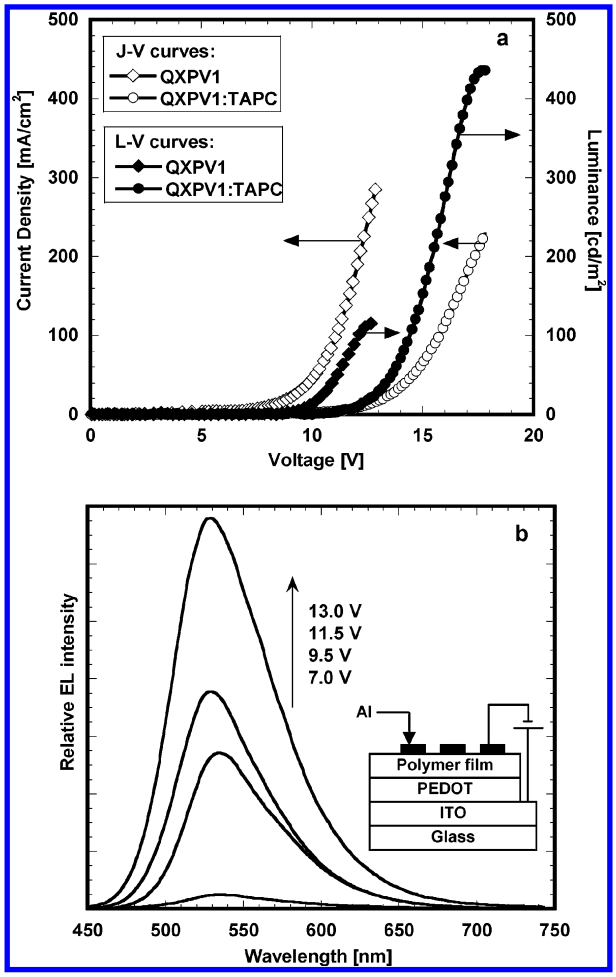

Figure 8. (a) Current density−voltage−luminance characteristics of LEDs from polymer **QXPV1** and its 95 wt % blend with TAPC. (b) EL spectra of the neat polymer device. The inset shows the device schematic.

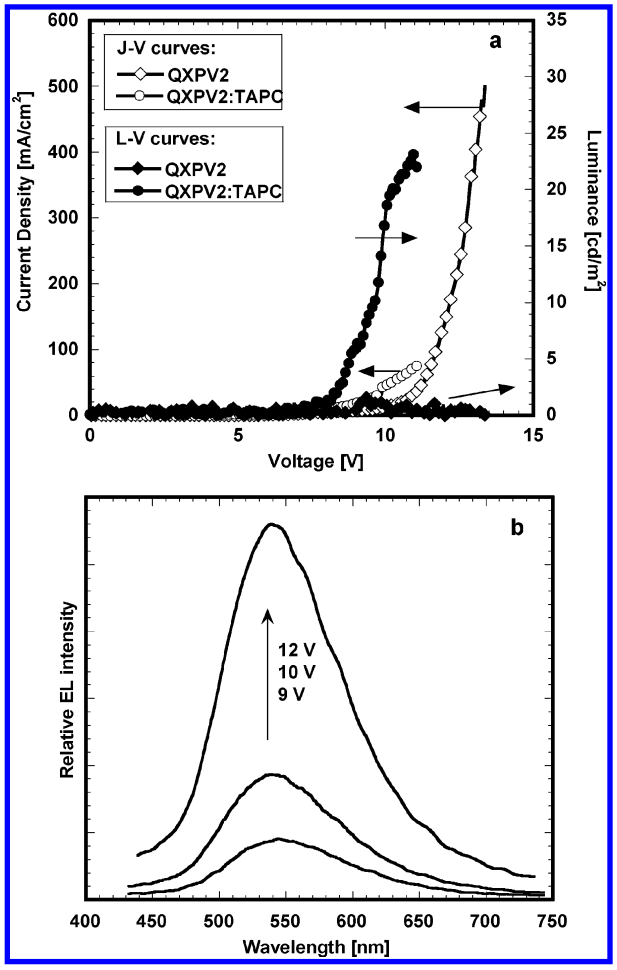

Figure 9. (a) Current density−voltage−luminance characteristics of LEDs from polymer **QXPV2** and its 95 wt % blend with TAPC. (b) EL spectra of the blend device.

single-layer LED is satisfactory, it could be further improved by adding appropriate charge transport materials. The irreversible oxidation in the CV of **QXPV1** (Figure 6a) suggests lack of bipolar character and poor hole transport that could limit the device performance. Thus, a blend of **QXPV1** was made with a hole transport molecule, 5 wt % 1,1-bis(di-4-tolylaminophenyl)cyclohexane (TAPC), to enhance the hole transport through the device. The $J-V-L$ characteristics of the corresponding LED are also shown in Figure 8a. A maximum brightness of 450 cd/m^2 and a maximum EQE of 0.06% at 17.5 V (435 cd/m^2, 225 mA/cm^2) were obtained, representing factors of 4−5 enhancement in performance compared to the **QXPV1** LED. Devices made from similar blends of **QXPV1** with a hole-transporting PVK polymer showed slightly lower efficiencies due to higher operating voltages. Further improvements in EL device efficiencies are likely by optimizing the blend composition. The EL spectra of the blend LED (not shown) are very similar to those of neat **QXPV1** with yellow-green emission at all voltages.

Figure 9a shows the $J-V-L$ characteristics of **QXPV2** LEDs, both neat polymer and blends with TAPC. The neat polymer device did not show any measurable luminance until 13 V even at the high current densities of 500 mA/cm^2, although the weak EL was visible to the eye. On addition of 5 wt % TAPC to **QXPV2**, a low brightness of 23 cd/m^2 was seen with EQE of 0.01% at 11 V (23 cd/m^2, 75 mA/cm^2). The EL spectra of the blend LED are shown in Figure 9b. The EL maxima were located at ∼538−543 nm and were comparable to the thin film PL maximum of **QXPV2** at 547 nm. It is rather surprising that although there is no significant difference in the EA/IP levels and electrochemical characteristics of **QXPV1** and **QXPV2**, the former is a much more emissive material than the latter. The poor performance of **QXPV2** as an emissive material in LEDs could be explained as being partly due to the very low fluorescence quantum yields in the solid state. Although the solid-state PL quantum yields were not calculated, we note that **QXPV1** had the highest PL quantum yield ($\phi_f = 0.55$) in solution among the series of polymers.

The LED characteristics of **QXPV3** are shown in Figure 10; part a shows the $J-V-L$ characteristics of **QXPV3** LEDs, and part b displays the EL spectra of the neat polymer diode. The neat polymer device had a low turn-on voltage of 4.0 V and a maximum brightness of 35 cd/m^2 at 12.0 V. The shape of the $J-V$ curve was typical of space-charge-limited currents in semiconductors with traps,[34] possibly due to poor electron injection and transport as evidenced by the inferior reduction characteristics in CV. The EL spectra of the neat LED shown in Figure 10b indicate yellow emission with maxima at 550 nm. A small improvement in device performance was obtained on addition of 5 wt % TAPC to **QXPV3**. The maximum brightness was 50 cd/m^2 with very low EQE of 0.004% at 11 V (48 cd/m^2, 420 mA/cm^2). As the IP of **QXPV3** is already low at 5.15 eV,

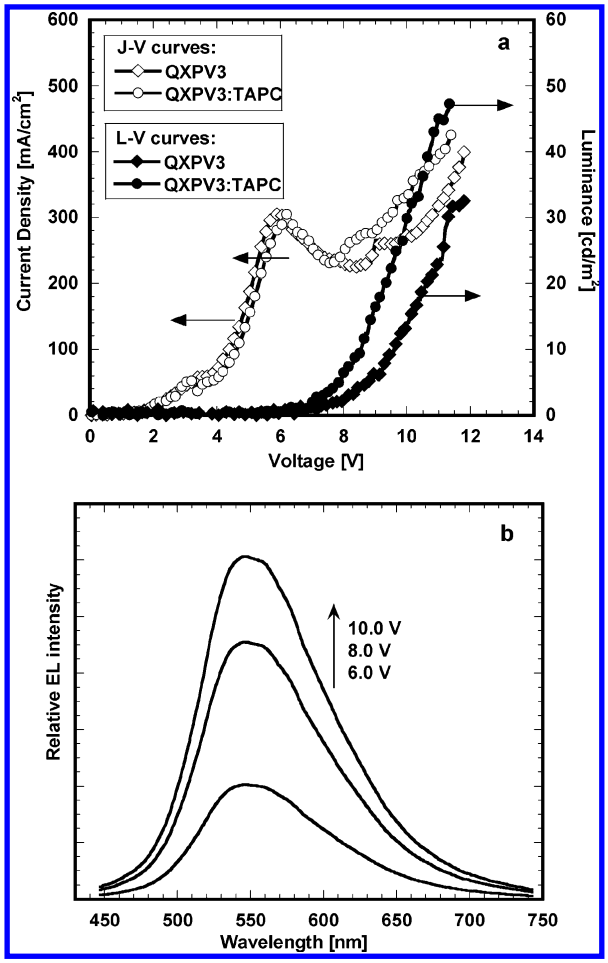

Figure 10. (a) Current density−voltage−luminance characteristics of LEDs from polymer **QXPV3** and its 95 wt % blend with TAPC. (b) EL spectra of the neat polymer device.

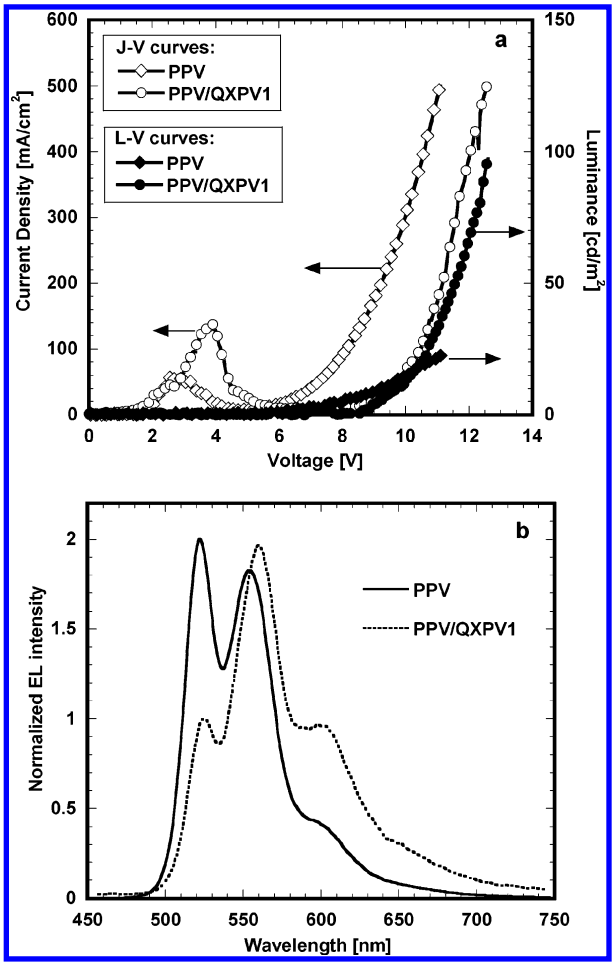

Figure 11. (a) Current density−voltage−luminance characteristics of LEDs from single-layer PPV and bilayer with **QXPV1**. (b) EL spectra of both devices at drive voltage of 11 V.

the addition of 5 wt % TAPC (IP = 5.3 eV) apparently did not improve hole transport in the diodes significantly.

In the case of polymer **QXPV4**, EL devices could not be fabricated due to the very poor film quality caused by the low solubility of the polymer in any solvent combination. Overall, polymer **QXPV1** with one quinoxaline moiety in the backbone is the best emissive material among the four quinoxaline-containing PPVs, most likely due to its high fluorescence quantum yield and good electron transport characteristics. To the best of our knowledge, this is one of the first systematic investigation of EL properties of quinoxaline-containing dialkoxy-PPVs. Compared to some previous studies on oxadiazole-containing PPVs, the present quinoxaline polymer **QXPV1** is much superior as an emissive material for LEDs.[10a,b,11] Besides, the good reversibility of the electrochemical reductions in **QXPV1** and **QXPV2** suggested that they could be used as electron-transport materials (ETMs) in conjunction with other p-type emissive polymers for multilayer LEDs.

The electron-transport properties of the quinoxaline−PPVs were investigated by fabricating bilayer LEDs of the type ITO/PPV/polymer/Al, with PPV serving as the emissive material. The $J-V-L$ characteristics of single-layer PPV and bilayer PPV LEDs with **QXPV1** are shown in Figure 11a. Single-layer PPV diodes had a maximum brightness of ~20 cd/m^2 and maximum EQE of 0.001% at 11 V (22 cd/m^2, 500 mA/cm^2). Enhancements in brightness and EQE by factors of 5 and 10, respectively, were obtained using a separate layer of **QXPV1**. The EL spectra of the two types of devices shown in Figure 11b show typical PPV emission with two well-resolved peaks at 522 and 555 nm, suggesting that **QXPV1** solely serves as the ETM with recombination occurring in the PPV layer. No enhancements in brightness were observed using **QXPV2** as an ETM, in spite of its similar energy levels to **QXPV1**. **QXPV3** did not work at all as an ETM with no measurable EL from the bilayer PPV/**QXPV3** LED. This suggests very poor electron transport properties of **QXPV3** as evidenced in its lack of reversibility in CV measurements. As an ETM for PPV-based LEDs, we note that **QXPV1** is inferior compared to previous polyquinoxalines[20] and some polyquinolines.[3b,4,6b] This could be explained as due to its poorer hole-blocking and electron-transport properties. The low IP of 5.28 eV in **QXPV1** does not present a significant barrier to hole injection at the PPV/**QXPV1** interface. Also, the electron mobilities through **QXPV1** would be much lower due to the long dodecyloxy side chains preventing efficient interchain hopping of charges. Both these factors were much improved in the conjugated rigid polyquinolines and polyquinoxalines leading to their superior performance as an ETM for PPV LEDs.

Conclusions

Four new dialkoxy-substituted poly(*p*-phenylenevinylene)s, containing one or two quinoxaline moieties

per repeat unit in the main chain or side chain, were prepared by Heck coupling of dibromoquinoxalines with 2,5-didodecyloxy-1,4-divinylbenzene. Polymers containing one quinoxaline moiety per repeat unit (**QXPV1** and **QXPV3**) displayed melting at low temperatures, while polymers with two quinoxalines per repeat unit (**QXPV2** and **QXPV4**) had high glass transition temperatures. The polymers emitted blue to green light (404−536 nm) in dilute chloroform solution and blue-green to yellow light (470−563 nm) in thin film. Time-resolved photoluminescence decay dynamics of the polymers revealed single-exponential lifetimes ranging from 200 ps to 2.2 ns in both dilute solution and thin film. Typical n-type characteristics were seen in polymers bearing quinoxaline moieties in the main chain (**QXPV1** and **QXPV2**) as revealed by their facile reversible reductions and irreversible oxidations in cyclic voltammetry. As emissive materials, greenish-yellow electroluminescence with a brightness of up to 450 cd/m^2 was obtained from single-layer blend LEDs of **QXPV1** with a triarylamine molecule. As electron transport materials in PPV bilayer LEDs, only moderate improvements in device performance were achieved. These results constitute the first systematic investigation of the photophysical and emissive properties of quinoxaline-containing PPV polymers for LED applications.

Acknowledgment. Work at the University of Washington was supported by the Army Research Office TOPS MURI (Grant DAAD19-01-1-0676).

References and Notes

(1) (a) Kraft, A.; Grimsdale, A. C.; Holmes, A. B. *Angew. Chem., Int. Ed.* **1998**, *37*, 402. (b) Friend, R. H.; Gymer, R. W.; Holmes, A. B.; Burroughes, J. H.; Marks, R. N.; Taliani, C.; Bradley, D. D. C.; Dos Santos, D. A.; Brédas, J. L.; Lögdlund, M.; Salaneck, W. R. *Nature (London)* **1999**, *397*, 121. (c) Rees, I. D.; Robinson, K. L.; Holmes, A. B.; Towns, C. R.; O'Dell, R. *MRS Bull.* **2002**, *27*, 451.

(2) (a) Rothberg, L. J.; Lovinger, A. J. *J. Mater. Res.* **1996**, *11*, 3174. (b) Heeger, A. J. *Solid State Commun.* **1998**, *107*, 673. (c) Sheats, J. R.; Antoniadis, H.; Hueschen, M.; Leonard, W.; Miller, J.; Moon, R.; Roitman, D.; Stocking, A. *Science* **1996**, *273*, 884.

(3) (a) Tarkka, R. M.; Zhang, X.; Jenekhe, S. A. *J. Am. Chem. Soc.* **1996**, *118*, 9438. (b) Zhang, X.; Shetty, A. S.; Jenekhe, S. A. *Macromolecules* **1999**, *32*, 7422.

(4) (a) Jenekhe, S. A.; Zhang, X.; Chen, X. L.; Choong, V.-E.; Gao, Y.; Hsieh, B. R. *Chem. Mater.* **1997**, *9*, 409. (b) Zhang, X.; Jenekhe, S. A. *Macromolecules* **2000**, *33*, 2069. (c) Tonzola, C. J.; Alam, M. M.; Jenekhe, S. A. *Adv. Mater.* **2002**, *14*, 1086.

(5) (a) Gustafsson, G.; Cao, Y.; Treacy, G. M.; Klavetter, F.; Colaneri, N.; Heeger, A. J. *Nature (London)* **1992**, *357*, 477. (b) Greenham, N. C.; Moratti, S. C.; Bradley, D. D. C.; Friend, R. H.; Holmes, A. B. *Nature (London)* **1993**, *365*, 628.

(6) (a) Zhu, Y.; Alam, M. M.; Jenekhe, S. A. *Macromolecules* **2002**, *35*, 9844. (b) Zhu, Y.; Alam, M. M.; Jenekhe, S. A. *Macromolecules* **2003**, *36*, 8958.

(7) (a) Tonzola, C. J.; Alam, M. M.; Kaminsky, W.; Jenekhe, S. A. *J. Am. Chem. Soc.* **2003**, *125*, 13548. (b) Alam, M. M.; Jenekhe, S. A. *Chem. Mater.* **2002**, *14*, 4775.

(8) (a) Fu, D.-K.; Xu, B.; Swager T. M. *Tetrahedron* **1997**, *53*, 15487. (b) Yang, W.; Huang, J.; Liu, C.; Niu, Y.; Hou, Q.; Yang, R.; Cao, Y. *Polymer* **2004**, *45*, 865.

(9) (a) Peng, Z.; Galvin, M. E. *Chem. Mater.* **1998**, *10*, 1785. (b) Liu, M. S.; Jiang, X.; Liu, S.; Herguth, P.; Jen, A. K.-Y. *Macromolecules* **2002**, *35*, 3532.

(10) (a) Peng, Z.; Bao, Z.; Galvin, M. E. *Adv. Mater.* **1998**, *10*, 680. (b) Bao, Z.; Peng, Z.; Galvin, M. E.; Chandross, E. A. *Chem. Mater.* **1993**, *5*, 1201. (c) Song, S.-Y.; Jang, M. S.; Shim, H.-K.; Hwang, D.-H.; Zyung, T. *Macromolecules* **1999**, *32*, 1482.

(11) (a) Mikroyannidis, J. A.; Spiliopoulos, I. K.; Kasimis, T. S.; Kulkarni, A. P.; Jenekhe, S. A. *Macromolecules* **2003**, *36*, 9295. (b) Mikroyannidis, J. A.; Spiliopoulos, I. K.; Kasimis, T. S.; Kulkarni, A. P.; Jenekhe, S. A. *J. Polym. Sci., Part A: Polym. Chem.* **2004**, *42*, 2112.

(12) (a) Zhan, X.; Liu, Y.; Wu, X.; Wang, S.; Zhu, D. *Macromolecules* **2002**, *35*, 2529. (b) Sun, Q.; Zhan, X.; Yang, C.; Liu, Y.; Li, Y.; Zhu, D. *Thin Solid Films* **2003**, *440*, 247.

(13) Jung, S. H.; Suh, D. H.; Cho, H. N. *Polym. Bull. (Berlin)* **2003**, *50*, 251.

(14) Jonforsen, M.; Johansson, T.; Inganas, O.; Andersson, M. R. *Macromolecules* **2002**, *35*, 1638.

(15) Lee, B. H.; Jaung, J. Y.; Cho, J.-W.; Yoon, K. J. *Polym. Bull. (Berlin)* **2003**, *50*, 9.

(16) Morin, J.-.F.; Leclerc, M. *Macromolecules* **2002**, *35*, 8413.

(17) (a) Kanbara, T.; Yamamoto, T. *Macromolecules* **1993**, *26*, 3464. (b) Yamamoto, T.; Sugiyama, K.; Kushida, T.; Inoue, T.; Kanbara, T. *J. Am. Chem. Soc.* **1996**, *118*, 3930.

(18) Jandke, M.; Strohriegl, P.; Berleb, S.; Werner, E.; Brütting, W. *Macromolecules* **1998**, *31*, 6434.

(19) Schmitz, C.; Pösch, P.; Thelakkat, M.; Schmidt, H.-W.; Montali, A.; Feldman, K.; Smith, P.; Weder, C. *Adv. Funct. Mater.* **2001**, *11*, 41.

(20) (a) Fukuda, T.; Kanbara, T.; Yamamoto, T.; Ishikawa, K.; Takezoe, H.; Fukuda, A. *Appl. Phys. Lett.* **1996**, *68*, 2346. (b) O'Brien, D.; Weaver, M. S.; Lidzey, D. G.; Bradley, D. D. C. *Appl. Phys. Lett.* **1996**, *69*, 881. (c) Cui, Y.; Zhang, X.; Jenekhe, S. A. *Macromolecules* **1999**, *32*, 3824.

(21) Heinrich, G.; Schoof, S.; Gusten, H. *J. Photochem.* **1974**, *3*, 315.

(22) (a) Kulkarni, A. P.; Jenekhe, S. A. *Macromolecules* **2003**, *36*, 5285. (b) Kulkarni, A. P.; Kong, X.; Jenekhe, S. A. *J. Phys. Chem. B.* **2004**, *108*, 8689.

(23) Goldfinger, M. B.; Crawford, K. B.; Swager, T. M. *J. Am. Chem. Soc.* **1997**, *119*, 4578.

(24) Ochoa, C.; Rodriguez, J. *J. Heterocycl. Chem.* **1997**, *34*, 1053.

(25) Kubel, C.; Chen, S. L.; Mullen, K. *Macromolecules* **1998**, *31*, 6014.

(26) McKillop, A.; Swann, B. P.; Ford, M. E.; Taylor, E. C. *J. Am. Chem. Soc.* **1973**, *95*, 3641.

(27) Tao, W.; Nesbitt, S.; Heck, R. F. *J. Org. Chem.* **1990**, *55*, 63.

(28) Srinivasan, N. S.; Lee, D. G. *J. Org. Chem.* **1979**, *44*, 1574.

(29) (a) Bao, Z.; Chen, Y.; Cai, R.; Yu, L. *Macromolecules* **1993**, *26*, 5281. (b) Vaidyanathan, S.; Dong, H.; Galvin, M. E. *Synth. Met.* **2004**, *142*, 1. (c) Brandon, K. L.; Bentley, P. G.; Bradley, D. D. C.; Dunmur, D. A. *Synth. Met.* **1997**, *91*, 305.

(30) (a) Samuel, I. D. W.; Rumbles, G.; Collison, C. J.; Friend, R. H.; Moratti, S. C.; Holmes, A. B. *Synth. Met.* **1997**, *84*, 497. (b) Smilowitz, L.; Hays, A.; Heeger, A. J.; Wang, G.; Bowers, J. E. *J. Chem. Phys.* **1993**, *98*, 6504.

(31) (a) Jenekhe, S. A.; Osaheni, J. A. *Science* **1994**, *265*, 765. (b) Osaheni, J. A.; Jenekhe, S. A. *Macromolecules* **1994**, *27*, 739.

(32) Jenekhe, S. A.; Lu, L.; Alam, M. M. *Macromolecules* **2001**, *34*, 7315.

(33) (a) Brédas, J. L.; Silbey, R.; Boudreaux, D. S.; Chance, R. R. *J. Am. Chem. Soc.* **1983**, *105*, 6555. (b) Agrawal, A. K.; Jenekhe, S. A. *Chem. Mater.* **1996**, *8*, 579.

(34) Campbell, A. J.; Bradley, D. D. C.; Lidzey, D. G. *J. Appl. Phys.* **1997**, *82*, 6326.

MA048903Q